THE EUROPEAN
PHYSICAL JOURNAL C

Evolution of strange and multi-strange hadron production with relative transverse multiplicity activity in underlying event

Prabhakar Palni[1,2,a] , **Arvind Khuntia**[3,b] , **Paolo Bartalini**[4,c]

[1] Faculty of Physics and Applied Computer Science, AGH University of Science and Technology, al. Mickiewicza 30, 30-059 Krakow, Poland
[2] *Present address*: Department of Physics, Goa University, Taleigao Plateau, Goa 403206, India
[3] H. Niewodniczanski Institute of Nuclear Physics, Polish Academy of Sciences, 31-342 Krakow, Poland
[4] Instituto de Ciencias Nucleares, Universidad Nacional Autonoma de Mexico, Apartado Postal 70-543, Mexico D.F. 04510, Mexico

Abstract In this work, the relative Underlying event (UE) transverse multiplicity activity classifier (R_T) is used to study the strange and multi-strange hadron production in proton-proton collisions. Our study with R_T would allow to disentangle these particles, which are originating from the soft and hard QCD processes. We have used the PYTHIA 8 Monte-Carlo (MC) with a different implementation of color reconnection and rope hadronization models to demonstrate the proton-proton collisions data at $\sqrt{s}$ = 13 TeV. The relative production of strange and multi-strange hadrons are discussed extensively in low and high transverse activity regions. In this contribution, the relative strange hadron production is enhanced with increasing R_T. This enhancement is significant for the strange baryons as compared to mesons. In addition, the particle ratios as a function of R_T confirm the baryon enhancement in new Color Reconnection (newCR), whereas the Rope model confirms the baryon enhancement only with strange quark content. Experimental confirmation of such results will provide more insight into the soft physics in the transverse region, which will be useful to investigate various tunes based on hadronization and color reconnection schemes.

1 Introduction

In recent times, the most important discoveries in proton-proton (pp) collisions are the evidence of collectivity [1–5] and strangeness enhancement [6–8]. They are remarkably similar to those observed in heavy-ion collisions at RHIC and LHC, where these features are attributed to the production of a deconfined hot and dense medium, known as the Quark–Gluon Plasma (QGP) [9,10]. The measurement of strange hadron production in minimum-bias pp collision at the LHC energies has shown an enhancement as a function of multiplicity density [6,11–14]. One of the important conclusions from that study was that most of the Quantum Chromodynamics (QCD) based MC models could not reproduce the data qualitatively. Strange quarks in pp collisions can be produced in the hard scattering via flavor excitation/creation and gluon splitting [15]. In soft scattering at low transverse momentum, strange quark pairs can be produced via nonperturbative processes. However, the production of strange quark being heavier is suppressed relative to hadrons containing only up and down quarks. The hadronic final states in minimum-bias events are the product of hard (perturbative) parton-parton scattering and soft scattering which is called the Underlying event (UE) [16–18]. The major contribution to the UE activity comes from the initial and final state radiation, beam-beam remnants, and PYTHIA specific physics processes such as multiple-parton interactions (MPI) in the same pp collision [19,20] and color reconnection (CR) [21].

MPI plays a significant role in the particle production at the LHC energies [7,22,23]. Measurements related to hadron yields in the minimum-bias (inelastic) collisions are convoluted with the hard scattering and the soft UE activity [24]. Most of the minimum-bias collisions at the LHC energies are soft, with a typical transverse momentum scale less than 2 GeV/c [25–28].

In this paper, we attempt to disentangle the hard QCD-process and investigate the hadron production. In particular, strange and multi-strange particles in the transverse region dominated by the soft QCD process. The novel relative transverse multiplicity variable (R_T) has an excellent discriminating power to probe collective effects in hadronization [29].

[a] e-mail: Prabhakar.Palni@cern.ch; Prabhakar.Palni@unigoa.ac.in (corresponding author)

[b] e-mail: Arvind.Khuntia@cern.ch

[c] e-mail: Paolo.Bartalini@cern.ch

Furthermore, the multiplicity distribution associated with the UE exhibits Koba–Nielsen–Olesen (KNO) scaling [30]. The relative transverse multiplicity variable, R_T, serves as a perfect tool to study the strange hadron production yield and transverse momentum spectra from low to high underlying event activity. The UE measurement with charged-particle jets showed dependence on the charged-particle jet radius, possibly due to the selection bias [31]. However, in this work, the highest transverse momentum charged-particle is used as a leading-object to define UE regions. The kinematical variables and acceptances are selected to match with ALICE detector [32] to compare results directly with the ALICE, which has an excellent particle identification capabilities. Neutral strange particle production in underlying event as a function of the leading p_T was first reported by CMS [33] in pp collision at $\sqrt{s} = 7$ TeV. These results showed constant strange to charged-particle ratios beyond the plateau region.

In the current study, PYTHIA 8 (version 8.301) MC event generator along with three different models that incorporate various color flow and hadronization mechanisms to qualitatively describe various aspects of the underlying event activity is used. The Monash 2013 tune (labeled as "Monash") [34] whose parameters are tuned to the latest LHC data (run I and II) is used as a reference model. In addition to particle decays and soft-QCD modeling, PYTHIA 8 features leading-logarithmic initial- and final-state parton showers, Lund string hadronization, and MPI models [35,36]. Furthermore, new QCD based color-space model, which allows strings to form between leading and non-leading color connected parton [37] is considered. When this model (which allows color-epsilon and anti-epsilon structure formation) is combined with PYTHIA's model for junction fragmentation [38], it gives rise to a new source of baryon production. This novel model (labeled as "newCR") can describe the average transverse momentum of charged-particles and also production rates of baryons. The third model (labeled as "Rope") is based on the rope hadronization formalism [39,40], which describes the interactions between the overlapping Lund strings in the transverse space to combine into color ropes. Such color ropes are expected to give more strange particles and baryons. In these models, the minimum-bias (inelastic) events are generated for proton-proton collision at the center of mass energy, $\sqrt{s} = 13$ TeV.

The outline of this paper is the following. In Sect. 2, we briefly describe the event selection criteria for UE and various observables under this study. The results are discussed in Sect. 3, based on the leading p_T and transverse multiplicity activity classifier, R_T. Finally, in Sect. 4, we summarize our findings and conclusions are drawn.
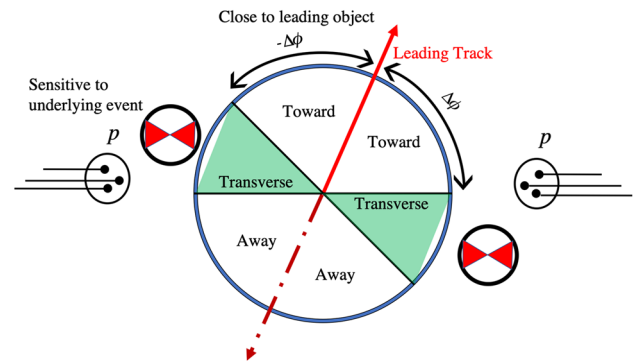
Fig. 1 Diagram illustrating the towards, transverse and away regions of the azimuthal angle with respect to the leading-charged particle in the typical pp collision event
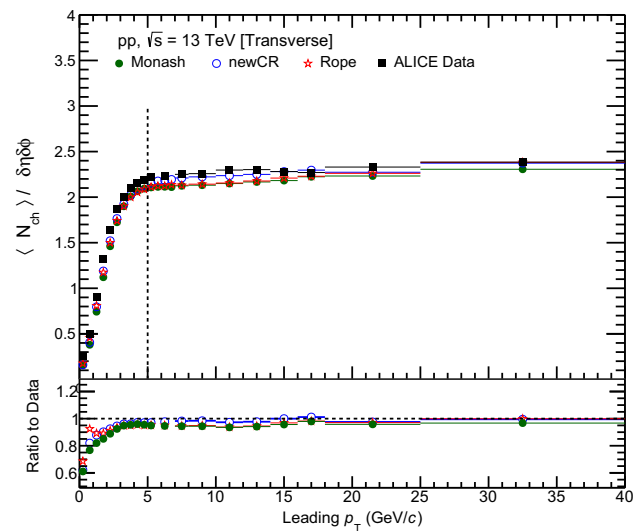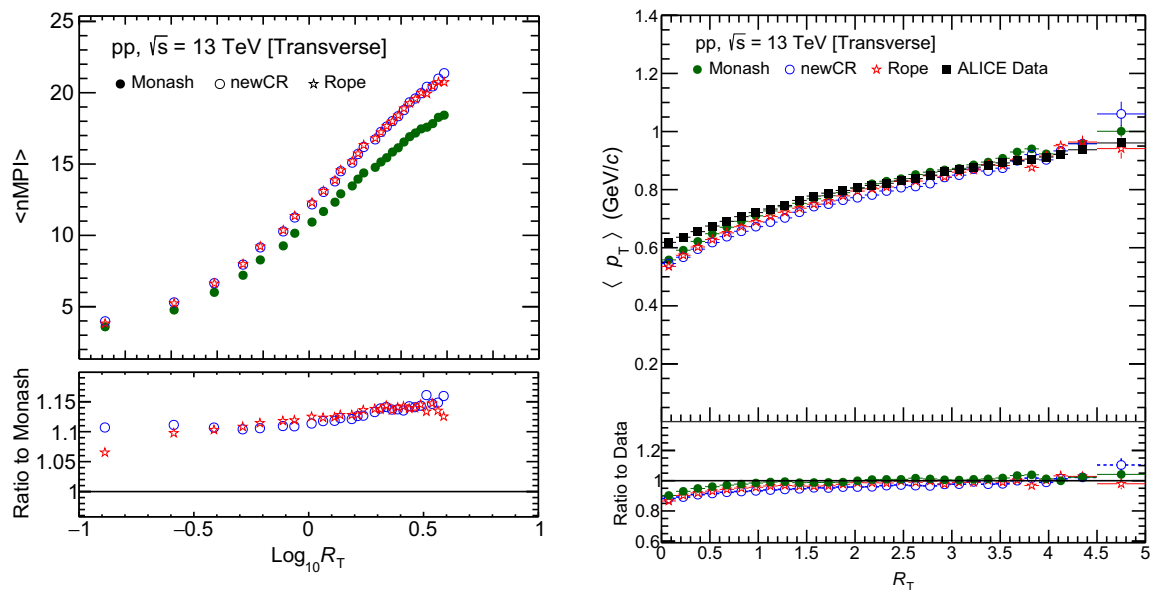

Fig. 2 The average number density of charged-particles as a function of leading p_T in the transverse region. The ALICE data are compared to three different models

2 Event selection and observables

The UE properties are derived based on the leading charged-particle direction in the event. This charged-particle is expected to have the direction of the parton produced with the highest transverse momentum in the hard scattering. The event is classified into three topological regions: (i) towards, (ii) away and (iii) transverse region in terms of the azimuthal angle difference, $\Delta\phi$, between the directions of the leading charged-particle and that of any other particle in the event as shown in Fig. 1. The particles produced in the towards region are spanned by the azimuthal angle $|\Delta\phi| < 60°$, and in the away region, $|\Delta\phi| > 120°$, which is expected to be dominated by the hard scatterings. The UE activity can be best studied in the transverse region, $60° < |\Delta\phi| < 120°$.

All the observables are measured using the primary charged-particle tracks with transverse momentum $p_T >$

Fig. 3 The average number of MPI in an event as a function of $\log_{10}(R_T)$ for transverse region (left panel). The $\langle p_T \rangle$ of charged-particles as a function of R_T for the transverse region (right panel)

0.15 GeV/c and absolute pseudo-rapidity, $|\eta| < 0.8$. The particles produced from the decay of hadrons with lifetime between $30 < \tau < 3000$ ps are considered as secondary particles. This study includes prompt neutral and charged strange hadrons (K_S^0, K^{*0}, ϕ, $\Lambda(\bar{\Lambda})$, $\Xi^{\pm}$, $\Omega^{\pm}$) with $p_T > 0.15$ GeV/c and $|\eta| < 0.8$.

Traditionally, observables such as average multiplicity of charged-particles or average scalar sum of charged-particles p_T per event are measured as a function of leading charged-particle track transverse momentum (p_T^{lead}). The charged-particle density in the transverse region rises steeply for low values of p_T^{lead} and reaches a plateau [41–43]. We have compared the charged-particle density measured by ALICE [41] in the transverse region to different PYTHIA 8 models as shown in the top panel of Fig. 2. Agreement between the ALICE data and the models are shown in the bottom panel. For p_T^{lead} below 2 GeV/c, all the three models under-predict the ALICE data, whereas in the plateau region differences between the data and models is below $\sim 8\%$ and independent of p_T^{lead}. The UE activity is classified in the plateau region ($5 < p_T^{lead} < 40$ GeV/c) to define relative transverse activity variable, R_T. In this region, all the models are in good agreement with the experimental data. The R_T is defined as the ratio of multiplicity of the inclusive charged-particles and identified strange hadrons (N_{inc}) to its event-averaged multiplicity ($\langle N_{inc} \rangle$) in the transverse region:

$$R_T = \frac{N_{inc}}{\langle N_{inc} \rangle} \tag{1}$$

The R_T variable is a useful tool to differentiate events with higher-than-average ($R_T > 1$) from lower-than-average

($R_T < 1$) UE activity, irrespective of the center of mass energy or any fiducial requirements on the observable. The event-averaged multiplicity, $\langle N_{inc} \rangle$, (and width) for "Monash", "newCR", and "Rope" models are 7.72 (4.94), 7.97 (4.94), and 7.65 (4.85), respectively. For comparing ALICE experimental data with MC models (as shown in Figs. 2 and 3 (right panel)), we have considered the charged-particles instead of N_{inc}.

3 Results and discussion

In this work, all the results are discussed by taking Monash as a reference model to understand the particle production mechanism with respect to newCR and Rope models. Figure 3 (left panel) shows average number of MPI in an event as a function of $\log_{10}(R_T)$ for the transverse region in three different models. The average number of MPI increases steeply with $\log_{10}(R_T)$ beyond 0, which corresponds to $R_T \sim 1$ and it is 10–15% higher for newCR and Rope models. The highest event activity at $\log_{10}(R_T) \simeq 0.5$ has twice the average number of MPI as compared to $\log_{10}(R_T) = 0$. The mean transverse momentum ($\langle p_T \rangle$) of the charged-particles as a function of R_T in the transverse region is compared among different MC models as shown in Fig. 3 (right panel). The $\langle p_T \rangle$ increases with R_T for all the three MC models and qualitatively explains the ALICE data. The color reconnection present in all the three models allows interaction between the strings which generates flow-like effects in the final state. An increase in the $\langle p_T \rangle$ with R_T is attributed to the presence of CR between the interacting strings. The ratio of ALICE

data to MC models is shown in the bottom panel of Fig. 3. The $\langle p_T \rangle$ is underestimated by all the three models by less than 10% below $R_T < 0.5$, whereas for $R_T > 3$, the trend is in agreement with the ALICE data [41]. A similar trend has been observed for the $\langle p_T \rangle$ as a function of charged-particle density in minimum bias events between the ALICE data [44] and Monash model.

The average ratios of production rates of the strange hadron to the average rates of the pions as a function of p_T^{lead} in the transverse region are shown in Fig. 4. To probe any sensitivity to the relative strangeness enhancement, the strange hadron yields are normalized to pion yields. Moreover, this ratio also factors out any contribution from differences in the overall multiplicity spectra of the tunes and MC models. The average strange particle production relative to pions increases significantly at low lead p_T, eventually reaching the plateau region at around 1–3 GeV/c. The average ratios for different particles are scaled by different factors to improve visibility. The similarity between production rates of strange hadrons ratios and charged-particles [41] as a function of p_T^{lead} confirms the impact-parameter picture of the multiple parton interactions in pp collisions, in which the centrality of the collision and the MPI activity are correlated. Strange hadrons with higher mass attain the plateau at higher leading p_T. The newCR and Rope models predict higher production of strange baryons as compared to strange mesons. The production rates of Ω ($|S| = 3$) with p_T^{lead} in the plateau region for newCR and Rope models are ~ 10 and ~ 3 times higher as compared to Monash, respectively. The relative yields are similar in the case of Λ and Ξ in the Rope model. However, higher production rates ($\sim 30\%$) are predicted in the newCR model for Λ as compared to Ξ.

The particle production in different p_T region has different origins and thus p_T-differential ratios provide a more differential understanding of particle production and hadronization. The p_T-differential ratio of the strange and multi-strange hadrons to pions in the transverse region for integrated R_T is shown in Fig. 5. A universal trend in the relative production of strange hadrons with p_T can be seen, which finally reaches a plateau beyond 2–4 GeV/c for all the three models. The plateau shifts towards the high p_T value for the heavier strange particles, which can be attributed to collectivity like effects originating from the color reconnection by boosting the emitted particles to higher momenta. Comparison with the Monash shows an increase in the strange meson production by (10–20 %) in p_T region 0.5–1.5 GeV/c as shown in Fig. 5 (left panel) for Rope model. However, in higher p_T region production rates in both Rope and newCR models are suppressed. Significant differences in strange baryons rates are observed among the MC models as shown in Fig. 5 (right panel). The magnitude is highest for the Ω, by up to a factor of 10 for the Rope, and 4 for the newCR model in the p_T region between 0 and 3 GeV/c. Comparison of the
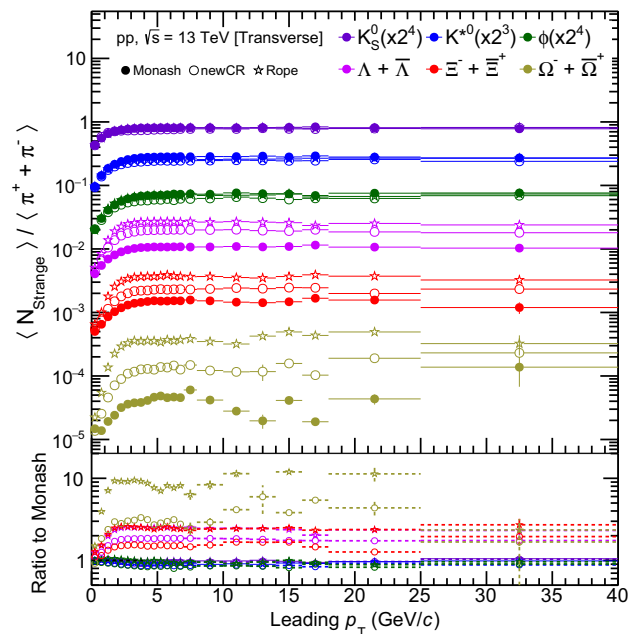

Fig. 4 Ratio of average strange hadrons to pions as a function of leading p_T in the transverse region

Rope and newCR models for Λ and Ξ show 2–3 times higher production rates in the p_T region 0–3 GeV/c. The behavior of the strange hadron production normalized to pions with R_T is a useful tool to understand different hadronization models. A comprehensive study has been performed for strange hadrons both in low ($R_T < 1$) and high R_T ($R_T > 1$) regions which correspond to low and high UE activity in the transverse region.

The ratio of average strange hadron yield to pions as shown in Fig. 6, increases with increasing R_T for all the MC models. This increase in yield ratios with R_T, particularly for $R_T > 1$ can be attributed to the higher multiple partonic interactions as shown in Fig. 3 (left panel). In the case of strange mesons, Monash shows higher production rates with R_T, whereas Rope and newCR model shows 10–15% less production. On the other hand, for strange baryons, enhancement is significantly higher as compared to mesons. The highest production rate is predicted for multi-strange baryon (Ω) in the Rope followed by newCR model. This trend is consistent with our earlier observation with leading p_T, as shown in Fig. 4. Enhancement in newCR as compared to Monash can be understood as an introduction of the junctions structure during the color reconnection phases, which favors the baryon enhancement over mesons. Further contribution to strange and multi-strange hadrons in the Rope model comes from additional production of strangeness and di-quarks due to interacting strings which form ropes and consequently hadronize.

The particle production chemistry in UE is investigated by measuring different particle yield ratios which are sensitive
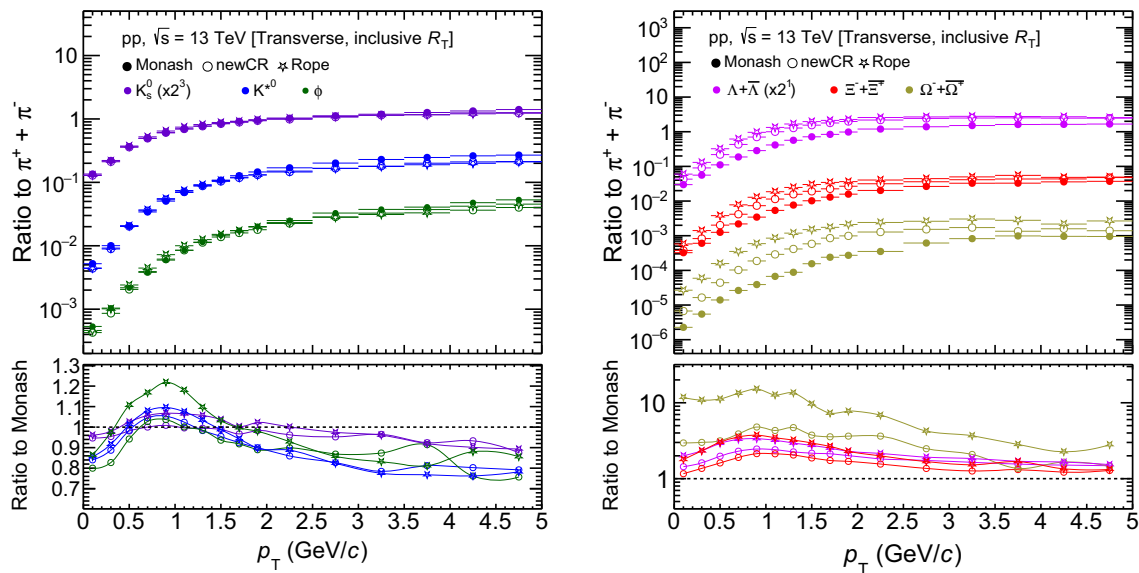
Fig. 5 p_T-differential ratios of strange mesons (left panel) and strange baryons (right panel) to pions for inclusive R_T in the transverse region. The p_T-differential ratios for K_S^0 and Λ are scaled by different factors to improve the visibility
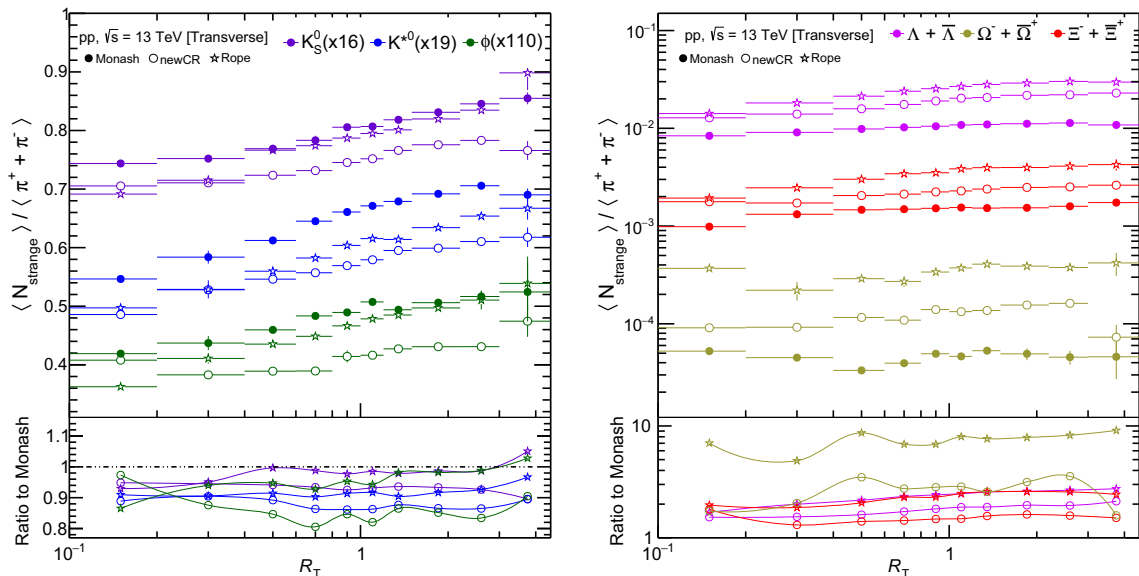
Fig. 6 Ratios of strange particles to pions as a function of R_T in the transverse region. The ratios of K_S^0, K^{*0} and ϕ are scaled by different factors for better visibility

to different hadron masses, baryon/meson, and strangeness content with R_T, as shown in Fig. 7. We observe dependence for baryon to meson ratios as a function of R_T for p/ϕ and Λ/K_S^0. The Λ/K_S^0 ratio has the highest production rate in the Rope model (~ 2.5 times) followed by newCR (~ 2 times) as compared to Monash in the high relative transverse activity region. The p/ϕ ratio obtained from the newCR and Rope models has similar production rate as proton being non-strange particles do not have further contributions from the Rope model. The individual particle yield increases with R_T, however, the effective baryon to baryon (Ξ/Λ) or meson to

meson (ϕ/K_S^0) ratios cancel-out, which results in the independent behavior with R_T.

4 Summary and conclusion

We have extensively studied the strange and multi-strange particle production in the transverse region as a function of leading p_T and transverse multiplicity activity in pp collisions at $\sqrt{s}$ = 13 TeV. Three different models with different implementation of hadronization and color reconnection are
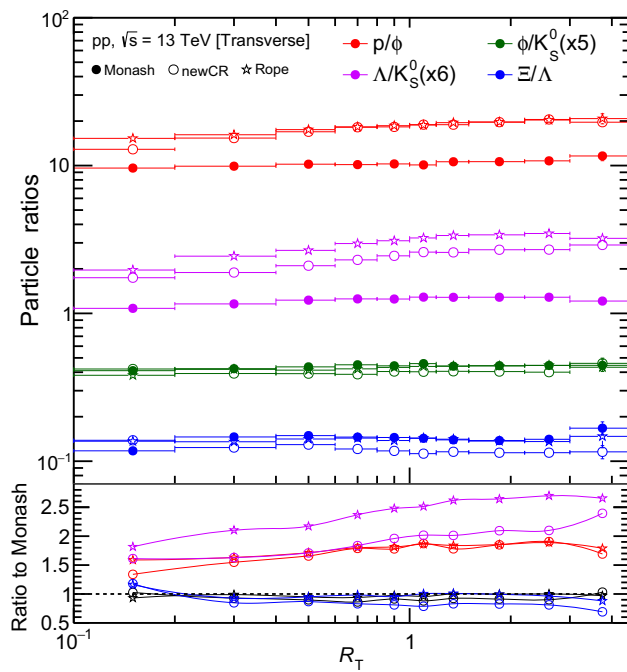
Fig. 7 An average hadron yield ratios as a function of R_T in the transverse region. The Λ/K_S^0 and ϕ/K_S^0 ratios are scaled by different factors to improve the visibility

used to study the dependence of the particle production in the transverse region using the PYTHIA 8 event generator. In this paper, an attempt has been made to disentangle the soft and hard QCD processes and to look into the particle production in a more differential manner using the transverse UE activity classifier, R_T. The newCR model includes baryon enhancement due to the junctions structure introduction during the color reconnection stage. Whereas Rope model incorporates strangeness enhancement due to surplus production of strangeness and di-quarks compared to Monash as a function of R_T. The steep rise of $\langle p_T \rangle$ in the transverse region as a function of R_T is qualitatively explained by all the three models. These models underestimate the $\langle p_T \rangle$ at low transverse activity region ($R_T < 1$) for the ALICE data, whereas it is in good agreement at higher R_T values. The average strange particle production relative to pions as a function of leading p_T increases significantly at low leading p_T, eventually reaching the plateau region at around 1–3 GeV/c. A systematic shift in the knee of the plateau towards the higher value of leading p_T with the heavier hadrons is observed. An enhancement of baryons relative to pions with leading p_T is predicted in the newCR model and additional production in the Rope model. The production rate of baryon with the highest strangeness, Ω, in the plateau region for newCR and Rope models is ~ 10 and ~ 3 times higher as compared to Monash, respectively. The p_T-differential particle ratios in the transverse region show the evolution of the spectral shape for both strange mesons and baryons in low-

p_T region between 0 and 3 GeV/c. A strong increased production of strange baryons in the newCR and Rope model around 1 GeV/c is observed. The ratio of average strange hadron yield to pions increases as a function of R_T in all the MC models. The Monash shows higher production rates with R_T for strange mesons, whereas the Rope and newCR models show higher production rates for strange baryons. The p/ϕ and Λ/K_S^0 ratios as a function of R_T confirms the baryon enhancement in newCR, whereas Rope model is responsible for baryon enhancement with strange quark content. Moreover, meson to meson and baryon to baryon ratios do not show a significant dependence on R_T.

Previous studies show that most of the MC models do not explain the enhancement of strange hadron production in pp collision as a function of charged-particle multiplicity density. Our study with the transverse multiplicity activity classifier provides qualitative evidence of an increase in strange hadron production in the underlying event. Experimental confirmation of these results will provide more insight into the soft physics in the transverse region as a function of R_T. This will further help to tune various hadronization and color reconnection schemes which can better explain particle production in pp collision.

Data Availability Statement This manuscript has no associated data or the data will not be deposited. [Authors' comment: This work includes all the necessary information in the manuscript.]

References

1. V. Khachatryan et al., CMS Collaboration. Phys. Lett. B **765**, 193 (2017). https://doi.org/10.1016/j.physletb.2016.12.009
2. B. Abelev et al., ALICE Collaboration. Phys. Lett. B **728**, 25–38 (2014). https://doi.org/10.1016/j.physletb.2013.11.020

3. A. Dumitru, K. Dusling, F. Gelis, J. Jalilian-Marian, T. Lappi, R. Venugopalan, Phys. Lett. B **697**, 21–25 (2011). https://doi.org/10.1016/j.physletb.2011.01.024
4. G.L. Ma, A. Bzdak, Phys. Lett. B **739**, 209 (2014). https://doi.org/10.1016/j.physletb.2014.10.066
5. A. Ortiz Velasquez, P. Christiansen, E. Cuautle Flores, I. Maldonado Cervantes, G. Paic, Phys. Rev. Lett. **111**, 042001 (2013). https://doi.org/10.1103/PhysRevLett.111.042001
6. J. Adam et al., ALICE Collaboration. Nature Phys. **13**, 535 (2017). https://doi.org/10.1038/nphys4111
7. P. Palni et al., ALICE Collaboration. Acta Phys. Polon. B **50**, 1185 (2019). https://doi.org/10.5506/APhysPolB.50.1185
8. A. Khuntia [ALICE Collaboration], arXiv:2001.09023 [hep-ex]
9. E.V. Shuryak, Phys. Rep. **61**, 71–158 (1980). https://doi.org/10.1016/0370-1573(80)90105-2
10. J. Rafelski, B. Muller, Phys. Rev. Lett. **56**, 2334 (1986). https://doi.org/10.1103/PhysRevLett.56.2334
11. S. Acharya et al., ALICE Collaboration. Eur. Phys. J. C **80**, 167 (2020). https://doi.org/10.1140/epjc/s10052-020-7673-8
12. V. Khachatryan et al., CMS Collaboration. JHEP **05**, 064 (2011). https://doi.org/10.1007/JHEP05(2011)064
13. S. Acharya et al., ALICE Collaboration. Phys. Rev. C **99**, 024906 (2019). https://doi.org/10.1103/PhysRevC.99.024906
14. K. Aamodt et al., ALICE Collaboration. Eur. Phys. J. C **71**, 1594 (2011). https://doi.org/10.1140/epjc/s10052-011-1594-5
15. J. Sollfrank, U.W. Heinz, Quark-Gluon Plasma **2**, 555–634 (1995). https://doi.org/10.1142/9789812830661_0010
16. R. Field, Acta Phys. Polon. B **42**, 2631 (2011). https://doi.org/10.5506/APhysPolB.42.2631
17. D. Acosta et al., CDF Collaboration. Phys. Rev. D **70**, 072002 (2004). https://doi.org/10.1103/PhysRevD.70.072002
18. D. Acosta et al., CDF Collaboration. Phys. Rev. D **65**, 092002 (2002). https://doi.org/10.1103/PhysRevD.65.092002
19. T. Sjöstrand, M. Zijl, Rev. D **36**, 2019 (1987). https://doi.org/10.1103/PhysRevD.36.2019Phys
20. P. Bartalini, J. Gaunt, Adv. Ser. Direct. High Energy Phys. **29**, 1–450 (2018). https://doi.org/10.1142/10646
21. T. Sjöstrand,. arXiv:1310.8073 [hep-ph]
22. B. Abelev et al., ALICE Collaboration. Phys. Lett. B **712**, 165 (2012). https://doi.org/10.1016/j.physletb.2012.04.052
23. D. Enterria, A. Snigirev, Phys. Lett. B **727**, 157 (2013). https://doi.org/10.1016/j.physletb.2013.10.004
24. E. Cuautle, R. Jimenez, I. Maldonado, A. Ortiz, G. Paic, E. Perez,. arXiv:1404.2372 [hep-ph]
25. B. Abelev et al., ALICE Collaboration. Phys. Lett. B **753**, 319 (2016). https://doi.org/10.1016/j.physletb.2015.12.030
26. G. Aad et al., ATLAS Collaboration. Phys. Lett. B **758**, 67 (2016). https://doi.org/10.1016/j.physletb.2016.04.050
27. V. Khachatryan et al., CMS Collaboration. Phys. Rev. Lett. **105**, 022002 (2010). https://doi.org/10.1103/PhysRevLett.105.022002
28. V. Khachatryan et al., CMS Collaboration. Eur. Phys. J. C **78**, 697 (2018). https://doi.org/10.1140/epjc/s10052-018-6144-y
29. T. Martin, P. Skands, S. Farrington, Eur. Phys. J. C **76**, 1 (2016). https://doi.org/10.1140/epjc/s10052-016-4135-4
30. A. Ortiz, L.V. Palomo, Phys. Rev. D **96**, 114019 (2017). https://doi.org/10.1103/PhysRevD.96.114019
31. G. Aad et al., ATLAS Collaboration. Phys. Rev. D **86**, 072004 (2012). https://doi.org/10.1103/PhysRevD.86.072004
32. K. Aamodt et al., ALICE Collaboration. JINST **3**, S08002 (2008). https://doi.org/10.1088/1748-0221/3/08/S08002
33. V. Khachatryan et al., CMS Collaboration. Phys. Rev. D **88**, 052001 (2013). https://doi.org/10.1103/PhysRevD.88.052001
34. P. Skands, S. Carrazza, J. Rojo, Eur. Phys. J. C **74**, 3024 (2014). https://doi.org/10.1140/epjc/s10052-014-3024-y
35. T. Sjostrand, S. Mrenna, P.Z. Skands, Comput. Phys. Commun. **178**, 852 (2008). https://doi.org/10.1016/j.cpc.2008.01.036
36. Pythia8 online manual http://home.thep.lu.se/~torbjorn/pythia81html/Welcome.html
37. J.R. Christiansen, P.Z. Skands, JHEP **08**, 003 (2015). https://doi.org/10.1007/JHEP08(2015)003
38. T. Sjostrand, P.Z. Skands, Nucl. Phys. B **659**, 243 (2003). https://doi.org/10.1016/S0550-3213(03)00193-7
39. C. Bierlich, J. Christiansen Phys. Rev. D **92**, 094010 (2015). https://doi.org/10.1103/PhysRevD.92.094010
40. T.S. Biro et al., Nucl. Phys. B **245**, 449–468 (1984). https://doi.org/10.1016/0550-3213(84)90441-3
41. B. Abelev et al. [ALICE Collaboration], **04**, 192 (2020). https://doi.org/10.1007/JHEP04(2020)192JHEP
42. M. Aaboud et al., ATLAS Collaboration. JHEP **03**, 157 (2017). https://doi.org/10.1007/JHEP03(2017)157
43. A. Sirunyan et al., CMS Collaboration. Eur. Phys. J. C **80**, 4 (2020). https://doi.org/10.1140/epjc/s10052-019-7499-4
44. S. Acharya et al., ALICE Collaboration. Eur. Phys. J. C **79**, 7350 (2019). https://doi.org/10.1140/epjc/s10052-019-7350-y